Soft probes of SU(5) unification

Ilia Gogoladze,[1,*] Rizwan Khalid,[1,†] Nobuchika Okada,[2,‡] and Qaisar Shafi[1]

[1]*Bartol Research Institute, Department of Physics and Astronomy, University of Delaware, Newark, Delaware 19716, USA*
[2]*Theory Group, KEK, Tsukuba 305-0801, Japan*

We explore the sparticle and Higgs spectroscopy of an SU(5) inspired extension of the constrained minimal supersymmetric standard model. The universal soft parameter m_0 is replaced by $m_{\bar{5}}$ and m_{10}, where $m_{\bar{5}}$ and m_{10} denote universal soft scalar masses associated with fields in the five- and ten-dimensional representations of SU(5). The special case $m_{\bar{5}} \ll m_{10}$ yields a rather characteristic sparticle spectroscopy, which can be tested at the LHC. We highlight a few benchmark points in which the lightest neutralino saturates the WMAP bound on cold dark matter abundance.

I. INTRODUCTION

With the imminent deployment of the Large Hadron Collider (LHC), a great deal of recent theoretical research has centered around the constrained minimal supersymmetric standard model (CMSSM). In contrast to a generic supersymmetric standard model, which can contain more than a hundred free parameters, the CMSSM contains just five, with three of them arising from supersymmetry (SUSY) breaking in the hidden sector, which is then transmitted to the visible sector through supergravity interactions [1]. These include m_0 and $m_{1/2}$, the universal soft scalar and gaugino masses, and A, the universal coefficient of the soft trilinear terms. The fourth parameter of the CMSSM is $\tan\beta$, the ratio between the vacuum expectations of the up- and down-type Higgs doublets in the MSSM. The fifth parameter is the sign of μ, which we will take to be positive in this paper.

The case for CMSSM [2] becomes even more compelling if account is taken of the apparent unification at $M_{\text{GUT}} \sim 2 \times 10^{16}$ GeV of the standard model gauge couplings, with SUSY broken around the TeV scale. In this case, the parameters m_0, $m_{1/2}$, and A are specified at M_{GUT}. By fixing these soft SUSY breaking terms, the relic abundance of neutralino dark matter can be predicted. The parameters determining this relic abundance are severely constrained by the most recent WMAP analysis [3].

Assuming that the universal soft SUSY breaking terms are prescribed at M_{GUT}, it is plausible that they carry some information about the underlying grand unified theory (GUT). For example, sparticles, which belong in a given representation of a GUT gauge group, can be expected to have identical soft masses at M_{GUT}. The sparticle masses at low scales are determined by the renormalization group equations (RGEs) of the various parameters. In the CMSSM the allowed parameter space, it appears, turns

out to be relatively restricted after the various phenomenological constraints are imposed. However, one should add that in some recent works it is claimed that the parameter space remains rather unconstrained [4].

In this paper, motivated by supersymmetric SU(5), we do not require identical sfermion masses at M_{GUT} for the $\bar{5}$ and 10 matter multiplets [5]. Instead, we introduce two distinct soft mass parameters at M_{GUT}, denoted as $m_{\bar{5}}$ and m_{10}. For simplicity, we also make the plausible assumption that $m_{\bar{5}}$ is also the asymptotic soft mass associated with the two Higgs supermultiplets 5 and $\bar{5}$ of SU(5). Note that we will not impose b-τ Yukawa unification, which follows from minimal SU(5), but which can be strongly violated, as we briefly show later, in the presence of higher dimensional operators. This will allow us to consider Higgs and sparticle spectroscopy without imposing additional restrictions on the parameters.

In what follows, we will investigate a generalized CMSSM inspired by SU(5) with the sfermion soft supersymmetry breaking (SSB) masses prescribed at M_{GUT} as follows:

$$m_{\tilde{D}^c} = m_{\tilde{L}} = m_{H_u} = m_{H_d} = m_{\bar{5}},$$
$$m_{\tilde{Q}} = m_{\tilde{U}^c} = m_{\tilde{E}^c} = m_{10}, \tag{1}$$

while the remaining parameters are the same as in the CMSSM. Clearly, the CMSSM is realized by setting $m_{\bar{5}} = m_{10} = m_0$.

Through this generalization, the resultant sparticle mass spectrum at the weak scale differs, as one should expect, from the CMSSM one. To see this, it is useful to examine the one-loop RGEs for the sparticle masses. For sfermion masses in the first and second generations, we can neglect Yukawa coupling contributions in the RGEs and to a good approximation, the analytic expressions (see [6] and references therein) are given by

$$m_{\tilde{Q}}^2 \simeq 4.3 m_{1/2}^2 + m_{10}^2, \qquad m_{\tilde{U}^c}^2 \simeq 3.9 m_{1/2}^2 + m_{10}^2,$$
$$m_{\tilde{D}^c}^2 \simeq 3.9 m_{1/2}^2 + m_{\bar{5}}^2, \qquad m_{\tilde{L}}^2 \simeq 0.47 m_{1/2}^2 + m_{\bar{5}}^2, \tag{2}$$
$$m_{\tilde{E}^c}^2 \simeq 0.15 m_{1/2}^2 + m_{10}^2,$$

---

*ilia@physics.udel.edu; On leave of absence from Andronikashvili Institute of Physics, GAS, 380077 Tbilisi, Georgia.
†rizwan@udel.edu
‡okadan@post.kek.jp

where for simplicity the sfermion masses are evaluated at 1 TeV. In these expressions, the terms proportional to $m_{1/2}$ are generated through RGEs, while $m_{\bar{5}}$ and m_{10} shift the overall value of sfermion squared masses. For $m_{\bar{5}}^2$, $m_{10}^2 \ll m_{1/2}^2$, the resultant sfermion masses are largely controlled by the gaugino masses and will be similar to the results in the CMSSM with $m_0^2 \ll m_{1/2}^2$. On the other hand, for $m_{\bar{5}}^2$ and/or $m_{10}^2 \gtrsim m_{1/2}^2$ and $m_{\bar{5}} \neq m_{10}$, we can see a remarkable difference. In particular, for slepton masses the gaugino mass contributions are not so large and as a result, the slepton mass spectrum can be dramatically different from the CMSSM results.

If the sparticles are discovered at the LHC and their masses measured, we can explore the nature of SUSY breaking by extrapolating, using RGEs, the masses toward high energies. As is easily understood from Eq. (2), the first and second generation sfermion masses from the $\bar{5}$ and **10** will show separate unification at M_{GUT}. This is in sharp contrast with the CMSSM, where all sfermion masses are unified into a single m_0. The boundary condition for the

FIG. 1 (color online). Evolution of the first two family sfermion masses ($m_{\tilde{Q}}$, $m_{\tilde{U}^c}$, $m_{\tilde{D}^c}$, $m_{\tilde{E}^c}$, and $m_{\tilde{L}}$, from top to bottom) in (a) SU(5), (b) CMSSM (where $m_{\tilde{U}^c} \simeq m_{\tilde{D}^c}$). Here, $m_{1/2} = 300$ GeV, $\tan\beta = 30$, $A_0 = 0$, and $\mu > 0$ for both cases, and $m_{\bar{5}} = 200$ GeV, $m_{10} = 300$ GeV for SU(5), while $m_0 = 300$ GeV for CMSSM.

sfermion masses in the CMSSM seems more appropriate for a GUT model based on SO(10) or E_6, where all the MSSM particles are embedded in a single representation. Thus, the soft masses can be used as a tool to probe the structure of the underlying GUT.

Figure 1 shows a schematic picture comparing unification of sfermion masses in an SU(5) inspired CMSSM model with the standard CMSSM. The running sfermion masses, computed to 1-loop, in the $\bar{5}$-plet and the **10**-plet are separately unified at M_{GUT} (Fig. 1(a)). The same figure for the CMSSM (or an SO(10)-like model) is shown in Fig. 1(b), where the soft masses converge to a single point at M_{GUT}. Note that in the following analysis we employ ISAJET, which computes the sparticle masses using the full 2-loop RGEs.

II. PHENOMENOLOGICAL CONSTRAINTS AND SCANNING PROCEDURE

We employ the ISAJET 7.78 package [7] to perform random scans over the parameter space. In this package, the weak scale values of gauge and third generation Yukawa couplings are evolved to M_{GUT} via the MSSM RGEs in the $\overline{DR}$ regularization scheme, where M_{GUT} is defined to be the scale at which $g_1 = g_2$. We do not enforce an exact unification of the strong coupling $g_3 = g_1 = g_2$ at M_{GUT}, since a few percent deviation from unification can be assigned to unknown GUT-scale threshold corrections [8]. At M_{GUT}, the boundary conditions presented in Eq. (1) are imposed and all the SSB parameters, along with the gauge and Yukawa couplings, are evolved back to the weak scale M_Z. In the evaluation of Yukawa couplings, the SUSY threshold corrections [9] are taken into account at the common scale $M_{\mathrm{SUSY}} = \sqrt{m_{\tilde{t}_L} m_{\tilde{t}_R}}$. The entire parameter set is iteratively run between M_Z and M_{GUT} using the full 2-loop RGEs until a stable solution is obtained. To better account for leading-log corrections, 1-loop step-beta functions are adopted for gauge and Yukawa couplings, and the SSB parameters m_i are extracted from RGEs at multiple scales $m_i = m_i(m_i)$. The RGE-improved 1-loop effective potential is minimized at an optimized scale M_{SUSY}, which effectively accounts for the leading 2-loop corrections. Full 1-loop radiative corrections are incorporated for all sparticle masses.

The requirement of radiative electroweak symmetry breaking [10] puts an important theoretical constraint on the parameter space. Another important constraint comes from limits on the cosmological abundance of stable charged particles [11]. This excludes regions in the parameter space where charged SUSY particles, such as $\tilde{\tau}_1$ or $\tilde{t}_1$, become the lightest supersymmetric particle (LSP). We accept only those solutions for which the neutralino is the LSP.

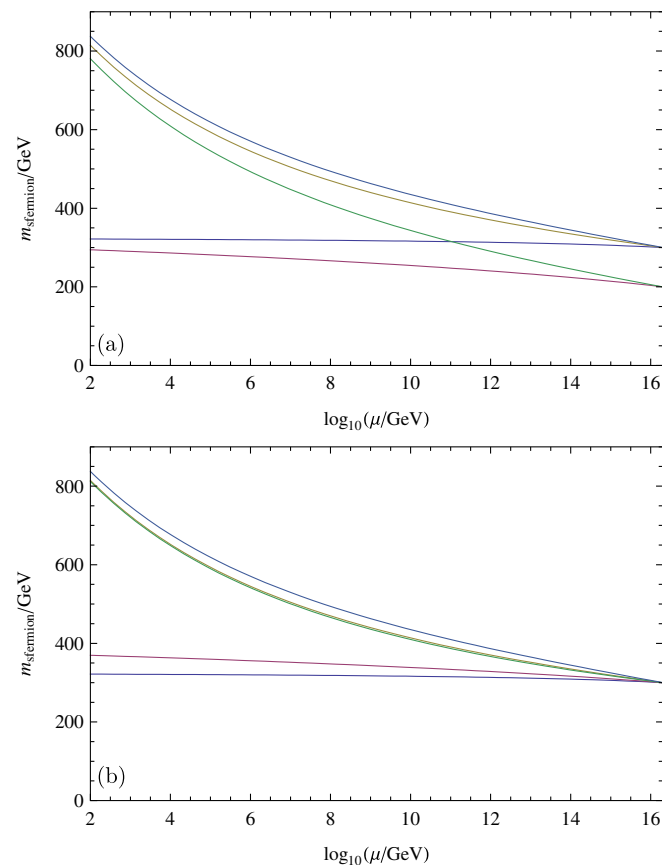We have performed random scans for the following parameter range:

$$0 \leq m_{\bar{5}} \leq 5 \text{ TeV},$$

$$0 \leq m_{10} \leq 5 \text{ TeV},$$

$$0 \leq m_{1/2} \leq 2 \text{ TeV}, \quad (3)$$

$$A_0 = 0.5 \text{ TeV}, 0, -1 \text{ TeV}, -2 \text{ TeV},$$

$$\tan\beta = 5, 10, 30, 50 \quad \text{and} \quad 55,$$

with $\mu > 0$ and $m_t = 172.6$ GeV [12].

After collecting the data, we use the ISATOOLS package [13] to implement the following phenomenological constraints:

$$m_{\tilde{W}_1}(\text{chargino mass}) \geq 103.5 \text{ GeV} \qquad [11],$$
$$m_h(\text{lightest Higgs mass}) \geq 114.4 \text{ GeV} \qquad [21],$$
$$BR(B_s \rightarrow \mu^+ \mu^-) < 5.8 \times 10^{-8} \qquad [22]$$
$$\Omega_{\text{CDM}} h^2 = 0.111^{+0.011}_{-0.015} \quad (2\sigma) \qquad [3],$$
$$2.85 \times 10^{-4} \leq BR(b \rightarrow s\gamma) \leq 4.24 \times 10^{-4} \quad (2\sigma) \quad [23],$$
$$(3.4 \times 10^{-10} \leq \Delta a_\mu \leq 55.6 \times 10^{-10} \quad (3\sigma) \quad [24].$$

We have collected 30 000 points for each set of A_0 and $\tan\beta$ values. All of these points satisfy the requirement of radiative electroweak symmetry breaking with the neutralino being the LSP in each case. Furthermore, all of these points satisfy an arbitrary constraint of $\Omega_{\text{CDM}} h^2 \leq 10$. This is done so as to collect more points with a WMAP acceptable value of cold dark matter relic abundance. We then successively apply the various experimental constraints on this data. First we apply the constraint on the $BR(B_s \rightarrow \mu^+ \mu^-)$, then the constraint on the chargino mass, followed by the WMAP upper bound on the relic density of cold dark matter. The constraint from $BR(b \rightarrow s\gamma)$ is then taken into consideration, followed by the constraint on Δa_μ. Finally, we apply also the lower bound on the dark matter relic abundance. The data is then plotted showing the successive application of each of these constraints.

The color coding is explained below, as well as in the Fig. 2 caption.

   (i) Black: Points excluded by the LEP 2 bound on the Higgs mass.
  (ii) Gray: Points that satisfy $BR(B_s \rightarrow \mu^+ \mu^-)$ and the chargino mass bound.
 (iii) Light green: Points that satisfy the WMAP upper bound on dark matter relic abundance.
  (iv) Dark green: Points that satisfy both upper and lower bounds on dark matter relic abundance.
   (v) Light and dark blue: Points that satisfy $BR(b \rightarrow s\gamma)$. Light blue points only satisfy the lower bound on dark matter relic abundance, while dark blue ones satisfy both upper and lower bounds.
  (vi) Orange and red: Points that satisfy the constraint from Δa_μ. Orange points satisfy only the lower bound on dark matter relic density, while red ones satisfy both the upper and lower bounds.

Thus, behind every red point, there is a dark blue, a dark green, and a gray point. Likewise, behind every orange point there is a light blue, a light green, and a gray point.
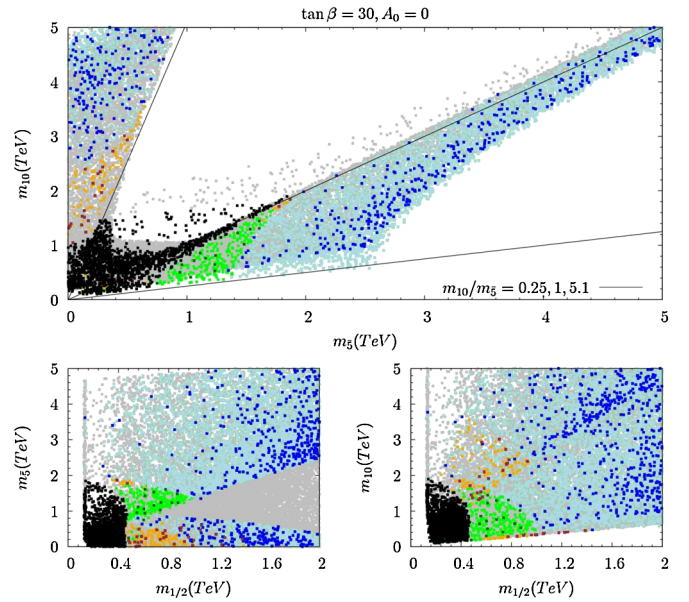

FIG. 2 (color online). Plots in $(m_{10}, m_{\bar{5}})$, $(m_{\bar{5}}, m_{1/2})$, and $(m_{10}, m_{1/2})$ planes for $\tan\beta = 30$, $A_0 = 0$, $\mu > 0$. The black region is excluded by the LEP 2 bound on the Higgs mass. Gray points satisfy constraints from $BR(B_s \rightarrow \mu^+ \mu^-)$ and the chargino mass bound. Light green points satisfy the WMAP upper bound on dark matter relic abundance. Dark green points satisfy both the upper and lower bounds on dark matter relic abundance. Light and dark blue points satisfy $BR(b \rightarrow s\gamma)$. Light blue points only satisfy the lower bound on dark matter relic abundance, while dark blue ones satisfy both upper and lower bounds. Orange and red points satisfy the constraint from Δa_μ. Orange points satisfy only the lower bound on dark matter relic density, while red ones satisfy both the upper and lower bounds.

III. b-τ (NON)-UNIFICATION

Before proceeding further, let us briefly discuss the issue of b-τ Yukawa unification. In minimal SU(5) with a single $5 + \bar{5}$ pair of Higgs, the Yukawa couplings of b and τ are equal at M_{GUT}. However, due to potentially large radiative corrections to the b mass [14], this asymptotic relation does not lead to a satisfactory prediction for the b quark mass without making additional assumptions about the soft masses, A terms and $\tan\beta$. Thus, in this paper we will not impose b-τ Yukawa unification at M_{GUT}. Indeed, one could expect this naive unification relation to be modified for a number of reasons. Consider the following b and τ Yukawa couplings (at M_{GUT}):

$$y 10_{\alpha\beta} \bar{5}^\alpha \bar{5}^\beta + \frac{\lambda_1}{\Lambda} 10_{\alpha\beta} \Sigma^\beta_\gamma \bar{5}^\gamma_f \bar{5}^\alpha_H + \frac{\lambda_2}{\Lambda} 10_{\alpha\beta} \Sigma^\beta_\gamma \bar{5}^\alpha_f \bar{5}^\gamma_H, \quad (4)$$

where Greek letters denote SU(5) indices, and the SU(5) adjoint Higgs Σ develops a vacuum expectation value (v), which breaks SU(5) to MSSM. We have included dimension-five terms in Eq. (4) to show how departure from b-τ unification can arise. Indeed, such higher order

terms have previously been used [15,16] to modify the "bad" Yukawa relations for the first two families predicted in minimal SU(5). The cutoff scale Λ can be the reduced Planck mass $M_{PL} = 2.4 \times 10^{18}$ GeV, or it can be a super-heavy mass scale of order M_{GUT}, associated with suitable vectorlike particles. (Integrating out these latter states should yield the desired dimension-five operators).

From Eq. (4), we find

$$y_b = y + \lambda_1(2\upsilon)/\Lambda + \lambda_2(-3\upsilon)/\Lambda$$
$$y_\tau = y + \lambda_1(-3\upsilon)/\Lambda + \lambda_2(-3\upsilon)/\Lambda. \tag{5}$$

For simplicity let us set $\lambda_2 = 0$, so that

$$y_b = y + 2y' \quad \text{and} \quad y_\tau = y - 3y', \tag{6}$$

where $y' = \lambda_1\upsilon/\Lambda$. These equations allow us to express y and y' in terms of y_b and y_τ:

$$y = (3y_b + 2y_\tau)/5 \quad \text{and} \quad y' = (y_b - y_\tau)/5. \tag{7}$$

With y_b and y_τ determined in conjunction with the various phenomenological constraints, the expressions in Eq. (7) provide the appropriate values for y and y'. Much of the viable parameter space obtained in this paper does not respect b-τ unification (see Fig. 11).

IV. RESULTS

Figure 2 shows the results in the $(m_{\bar{5}}, m_{10})$, $(m_{1/2}, m_{10})$, and $(m_{1/2}, m_{\bar{5}})$ planes for $\tan\beta = 30$, $A_0 = 0$, and $\mu > 0$. In the $(m_{\bar{5}}, m_{10})$ plane, lines corresponding to fixed ratios of $m_{10}/m_{\bar{5}} = 0.25$, 1, and 5.1 are plotted in Fig. 2 as a reference. Interestingly, we can see that the allowed region satisfying all the constraints is very limited, with wide excluded regions appearing in white. In the white region between the lines $1 \lesssim m_{10}/m_{\bar{5}} \lesssim 5.1$, the neutralino LSP is binolike, and its relic abundance is too large to be consistent with WMAP data. The lighter stau is the LSP (which can even be tachyonic) in the white region below the line $m_{10}/m_{\bar{5}} \simeq 0.25$. The white region for $m_{\bar{5}} \gtrsim 2.5$ TeV and below the line $m_{10}/m_{\bar{5}} = 1$ is excluded since no radiative electroweak symmetry breaking occurs there. In the $(m_{1/2}, m_{10})$ and $(m_{1/2}, m_{\bar{5}})$ planes, the region with $m_{1/2} \lesssim 0.15$ TeV is excluded since no radiative electroweak symmetry breaking occurs there. The region with a small m_{10} in the $(m_{1/2}, m_{10})$ plane is excluded because the lighter stau is the LSP (which can even be tachyonic). Similar remarks hold for Figs. 3–7, which show analogous plots for different values of $\tan\beta$ and A_0.

Figure 8 shows the effect of varying the top quark mass on the allowed parameter space. This is done in light of the sensitivity of the relic density prediction on the top quark mass as reported in [17] for the focus point region. We show the results in the $(m_{\bar{5}}, m_{10})$ plane with $m_t = 174$ GeV (top), $m_t = 172.6$ GeV (middle) and $m_t = 171.2$ GeV (bottom) for $\tan\beta = 30$, $A_0 = -1$ TeV (left panel) and $\tan\beta = 30$, $A_0 = 0$ (right panel). It is clear that while the
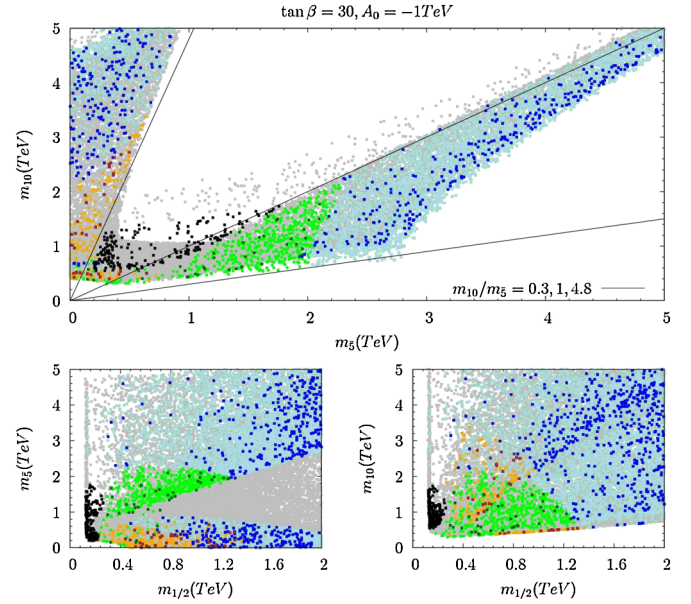

FIG. 3 (color online). Plots in $(m_{10}, m_{\bar{5}})$, $(m_{\bar{5}}, m_{1/2})$, $(m_{10}, m_{1/2})$ planes for $\tan\beta = 30$, $A_0 = -1$ TeV, $\mu > 0$. Color coding same as in Fig. 2.

allowed region does change somewhat, the interesting parameter space region where $m_{10} \neq m_{\bar{5}}$ continues to provide a solution that is characteristically different from the CMSSM.

Figure 9 shows the results in the $(m_{1/2}, m_{\bar{5}})$ plane for several fixed values of $m_{10}/m_{\bar{5}}$, with $\tan\beta = 50$, $A_0 = 0$, and $\mu > 0$. Let us examine Fig. 9(d) in more detail, which exhibits the case $m_{10} \gg m_{\bar{5}}$. The red and blue dots show
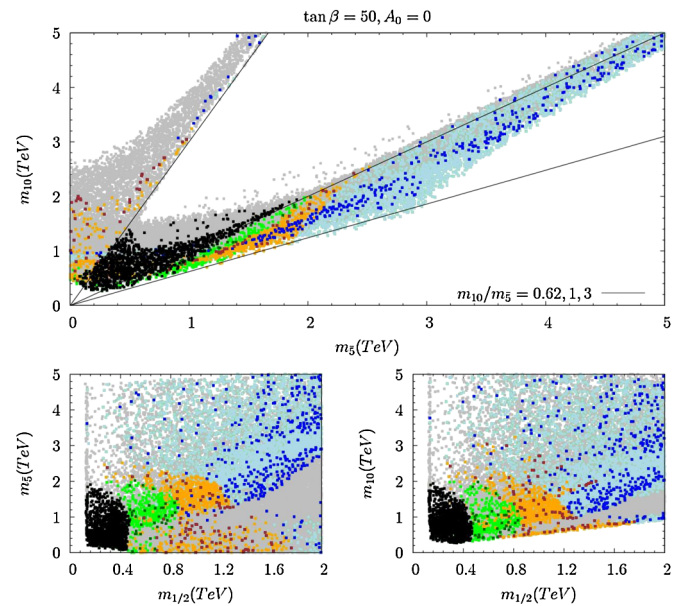

FIG. 4 (color online). Plots in $(m_{10}, m_{\bar{5}})$, $(m_{\bar{5}}, m_{1/2})$, $(m_{10}, m_{1/2})$ planes for $\tan\beta = 50$, $A_0 = 0$, $\mu > 0$. Color coding same as in Fig. 2.
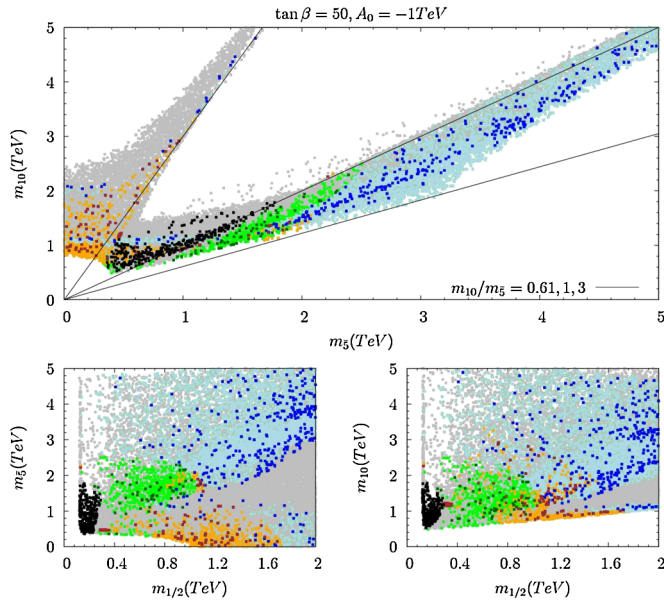
FIG. 5 (color online). Plots in $(m_{10}, m_{\bar{5}})$, $(m_{\bar{5}}, m_{1/2})$, $(m_{10}, m_{1/2})$ planes for $\tan\beta = 50$, $A_0 = -1$ TeV, $\mu > 0$. Color coding same as in Fig. 2.
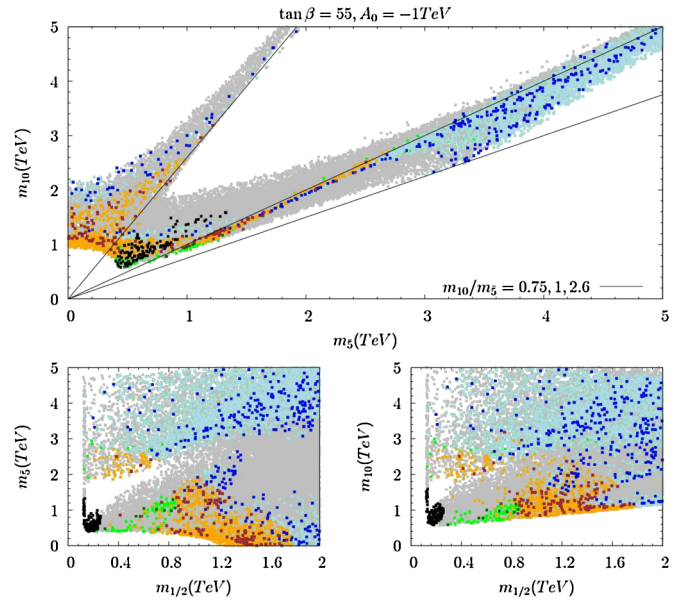
the allowed parameter sets (red dots are favored by the muon $g - 2$ experiments), and there are two branches for the allowed regions. The white regions in upper-left and in lower-right corners are excluded since the lighter stau is the LSP (it can even be tachyonic). The central region is excluded due to overabundance of the neutralino LSP. In both the allowed branches, the neutralino LSP is binolike and quasidegenerate with the lighter stau. Therefore, the
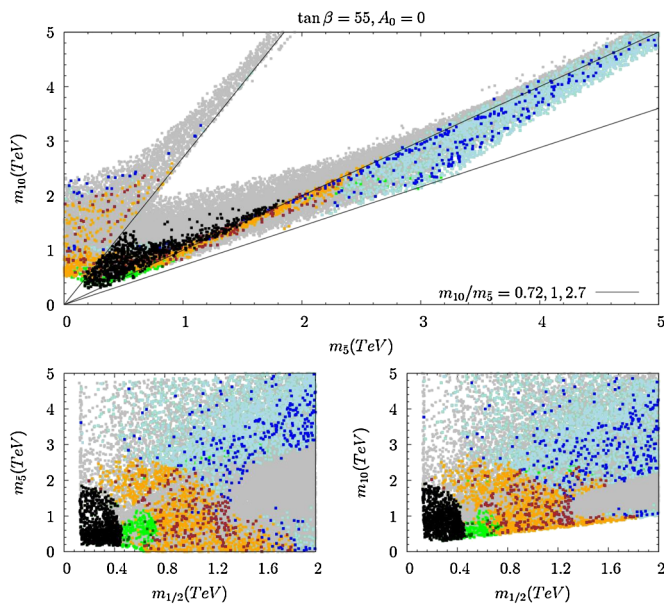

FIG. 6 (color online). Plots in $(m_{10}, m_{\bar{5}})$, $(m_{\bar{5}}, m_{1/2})$, $(m_{10}, m_{1/2})$ planes for $\tan\beta = 55$, $A_0 = 0$, $\mu > 0$. Color coding same as in Fig. 2.

FIG. 7 (color online). Plots in $(m_{10}, m_{\bar{5}})$, $(m_{\bar{5}}, m_{1/2})$, $(m_{10}, m_{1/2})$ planes for $\tan\beta = 55$, $A_0 = -1$ TeV, $\mu > 0$. Color coding same as in Fig. 2.

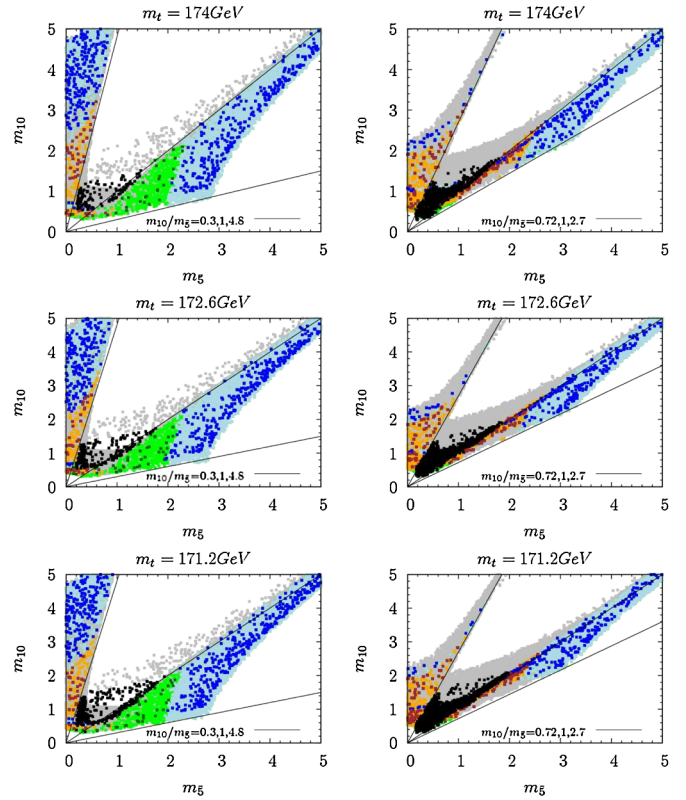FIG. 8 (color online). $(m_{\bar{5}}, m_{1/2})$ plane for $\tan\beta = 30$, $A_0 = -1$ TeV (left panel) and $\tan\beta = 55$, $A_0 = 0$ (right panel) with $\mu > 0$ showing the effect of varying the top quark mass. Color coding same as in Fig. 2.
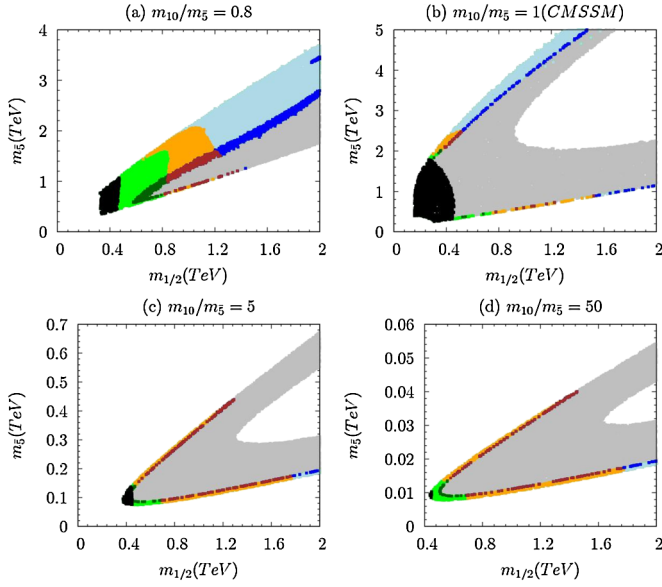
FIG. 9 (color online). $(m_{\bar{5}}, m_{1/2})$ plane for $\tan\beta = 50$, $A_0 = 0$, $\mu > 0$ with $m_{10}/m_{\bar{5}} = 0.8$, 1 (CMSSM), 5, and 50. Color coding same as in Fig. 2.

allowed region is the so-called coannihilation region in the CMSSM setup. However, there is a crucial difference in the composition of the lighter stau. In the lower branch, the lighter stau is mostly the right-handed stau as in the CMSSM, while it is mostly a left-handed stau in the upper branch. This is because in the upper branch m_{10} is large, so that the right-handed stau in the SU(5) **10**-plet is heavy. As a result, the relic abundance of the binolike neutralino can be consistent with the WMAP data through the coannihilation process with the mostly left-handed stau. This scenario is absent in the CMSSM, but is very characteristic for our SU(5) inspired MSSM.

Next, we select benchmark points from each of the allowed branches and compare the sparticle and Higgs boson masses with those in the CMSSM. The results are shown in Table I, together with the neutralino relic abundance and the spin-independent cross sections for neutralino-nucleon (proton and neutron) scattering. For comparison with the CMSSM, we fix $m_0 = m_{10}$, with all other parameters the same. We can see sizable differences in the sparticle mass spectra between the SU(5) model and the CMSSM. In particular, the difference is remarkable for the parameter set in the upper branch because of $m_{10} = m_0 > m_{1/2} \gg m_{\bar{5}}$. The sfermions in the $\bar{\bf 5}$ representation of SU(5) are much lighter than the corresponding sparticles in the CMSSM. The neutralino-nucleon cross sections are a few orders of magnitude smaller than the exclusion limits given by the current experiments for direct dark matter detection such as CDMS [18] and XENON10 [19].

Let us display other characteristic results of our model with a different set of input parameters, in particular, a

TABLE I. Sparticle and Higgs masses (in units of GeV), with $m_t = 172.6$ GeV, $\tan\beta = 50$, and $\mu > 0$. We present two SU(5) benchmark points and the corresponding CMSSM points for comparison. Also included are the spin-independent neutralino-nucleon interaction cross sections. Note that $2y_b \approx y_\tau$ at M_{GUT}.

	SU(5)	CMSSM	SU(5)	CMSSM
$m_{1/2}$	780	780	788	788
$m_{\bar{5}}$	9.66	483	20.9	1047
m_{10}	483	483	1047	1047
$\tan\beta$	50	50	50	50
A_0	0	0	0	0
m_h	117	117	118	117
m_H	798	767	1032	879
m_A	793	752	1026	874
$m_{H^\pm}$	802	762	1036	884
$m_{\tilde{\chi}^\pm_{1,2}}$	624, 990	624, 907	637, 1237	635, 885
$m_{\tilde{\chi}^0_{1,2,3,4}}$	330, 623, 981, 989	330, 623, 896, 924	336, 636, 1232, 1236	336, 634, 873, 885
$m_{\tilde{g}}$	1743	1748	1784	1796
$m_{\tilde{u}_{1,2}}$	1597, 1654	1597, 1655	1857, 1906	1857, 1905
$m_{\tilde{t}_{1,2}}$	1286, 1506	1265, 1487	1483, 1721	1399, 1639
$m_{\tilde{d}_{1,2}}$	1511, 1656	1591, 1657	1512, 1907	1851, 1906
$m_{\tilde{b}_{1,2}}$	1367, 1486	1412, 1482	1367, 1698	1593, 1662
$m_{\tilde{\nu}_{1,2,3}}$	515, 515, 450	705, 705, 639	513, 513, 358	1166, 1166, 1030
$m_{\tilde{e}_{1,2}}$	524, 563	563, 711	525, 1086	1086, 1169
$m_{\tilde{\tau}_{1,2}}$	354, 511	338, 661	349, 957	750, 1030
$\Omega_{\mathrm{CDM}}h^2$	0.115	0.053	0.118	0.175
$y_b/y_\tau(M_{\mathrm{GUT}})$	0.52	0.55	0.49	0.58
$\sigma_{\tilde{\chi}^0_1-p,\mathrm{SI}}$(pb)	4.00×10^{-10}	6.00×10^{-10}	1.13×10^{-10}	4.64×10^{-10}
$\sigma_{\tilde{\chi}^0_1-n,\mathrm{SI}}$(pb)	4.29×10^{-10}	6.45×10^{-10}	1.21×10^{-10}	4.96×10^{-10}

TABLE II. Sparticle and Higgs mass spectra (in units of GeV) for two additional SU(5) benchmark points (compare Table I), with $m_t = 172.6$ GeV and $\mu > 0$. The CMSSM equivalent of the first point is also included. The CMSSM equivalent of the second point gives tachyonic solutions and is therefore omitted. Also included are the spin-independent neutralino-nucleon interaction cross sections.

	SU(5)	CMSSM	SU(5)
$m_{1/2}$	287	287	275
$m_{\bar{5}}$	475	1203	73.9
m_{10}	1203	1203	850
$\tan\beta$	50	50	10
A_0	-1000	-1000	-2000
m_h	115	115	119
m_H	894	602	1130
m_A	888	598	1123
$m_{H^\pm}$	898	609	1133
$m_{\tilde{\chi}^\pm_{1,2}}$	236, 1059	232, 525	222, 1124
$m_{\tilde{\chi}^0_{1,2,3,4}}$	121, 236, 1055, 1058	120, 232, 515, 525	115, 223, 1110, 1121
$m_{\tilde{g}}$	746	757	696
$m_{\tilde{u}_{1,2}}$	1336, 1342	1333, 1338	1026, 1036
$m_{\tilde{t}_{1,2}}$	926, 1143	780, 984	366, 853
$m_{\tilde{d}_{1,2}}$	743, 1345	1334, 1341	571, 1039
$m_{\tilde{b}_{1,2}}$	554, 1121	947, 1065	542, 811
$m_{\tilde{\nu}_{1,2,3}}$	497, 497, 142	1214, 1214, 1041	175, 175, 120
$m_{\tilde{e}_{1,2}}$	506, 1208	1207, 1217	203, 857
$m_{\tilde{\tau}_{1,2}}$	130, 998	816, 1045	151, 839
$\Omega_{\mathrm{CDM}}h^2$	0.105	3.78	0.106
$y_b/y_\tau(M_{\mathrm{GUT}})$	0.44	0.64	0.64
$\sigma_{\tilde{\chi}^0_1-p,\mathrm{SI}}$(pb)	2.69×10^{-10}	2.80×10^{-9}	4.57×10^{-11}
$\sigma_{\tilde{\chi}^0_1-n,\mathrm{SI}}$(pb)	2.91×10^{-10}	3.04×10^{-9}	4.81×10^{-11}

nonzero A_0. Two cases are shown in Table II, together with a corresponding CMSSM result for $m_0 = m_{10}$. There is no phenomenologically viable solution in the CMSSM corresponding to the second case (the 4th column), since a lighter stop is found to be tachyonic in the CMSSM. In both SU(5) examples, the input $m_{1/2}$ values are relatively small, and as a result, all gauginos (gluino, gauginolike chargino, and gauginolike neutralinos) are relatively light compared to squarks. In the CMSSM, a small $m_{1/2}$ input, say, $m_{1/2} \lesssim 300$ GeV is excluded by the LEP 2 bound on the lightest Higgs boson mass, unless m_0 is large, $m_0 \gtrsim 1$ TeV. This is because the radiative corrections to the lightest Higgs boson mass via a heavy stop are necessary to make the Higgs boson mass (which is lighter than Z-boson mass at tree level) higher than the LEP 2 bound. Although the situation is the same for our model and the mass of **10**-plet including stops should be large, sfermions in $\bar{\mathbf{5}}$-plet can be (much) lighter than those in **10**-plet, and still be consistent with the phenomenological constraints.

In both cases, the relic abundance of the neutralino LSP matches the WMAP data and thus the neutralino can be the dominant component of cold dark matter in the present Universe. Since the neutralino is binolike, the coannihilation process with a quasidegenerate tau-sneutrino plays a crucial role in order to yield an appropriate relic abundance. Again, this case is not realized in the CMSSM. In

general, if the input values of $m_{1/2}$ and $m_{\bar{5}}$ are relatively small compared to m_{10}, the tau sneutrino is likely to be the next to LSP.

Table II shows that some of the colored sparticles can be light: Gluino and right-handed down-type squarks are light because of the small $m_{1/2}$ and $m_{\bar{5}}$ input values. The large value of A_0 input leads to a large mass splitting in stop mass eigenvalues. In the second case (the 4th column), in particular, the lightest stop is remarkably light. If gluinos are copiously produced at the LHC, gluino decays into the third generation squarks provide top quarks in the final state. Studies of this process may reveal a sparticle nature related to the third generation squarks [20]. For the second SU(5) case (the 4th column in Table II), the lighter stop is sufficiently light, so that its dominant decay mode is into a top quark and neutralino LSP, while the branching ratio to this process in the CMSSM is small. This process is certainly worth investigating at the LHC.

Let us briefly mention the A-funnel region that we observe in our model. Figure 10 shows plots in the $(m_{\tilde{\chi}^0_1}, m_A)$ plane with $A_0 = 0$ and $\tan\beta = 10$, 30, 50, and 55. Also shown in each case is the line $m_A = 2m_{\tilde{\chi}^0_1}$ from which we find that the A-funnel region appears for $\tan\beta = 50$ and 55, where neutralinos can annihilate via the CP-odd (H_A) and CP-even (H) Higgs bosons.
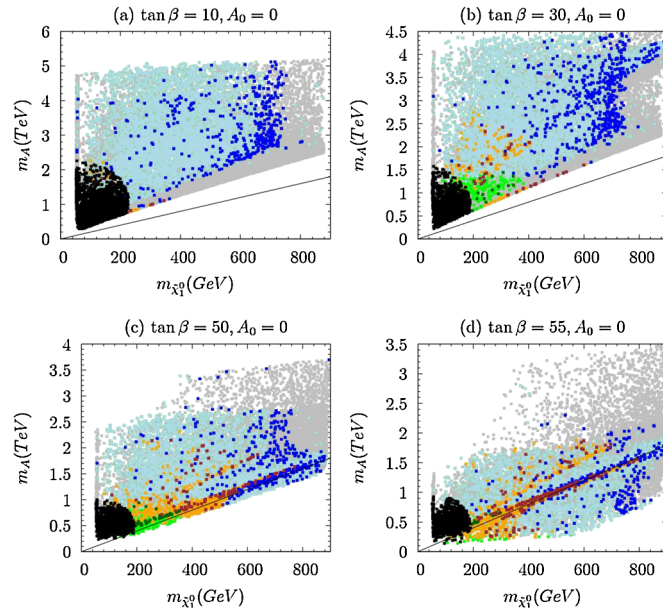
FIG. 10 (color online). Plots in $(m_A, m_{\tilde{\chi}_1^0})$ plane with $A_0 = 0$, $\mu > 0$ and $\tan\beta = 10, 30, 50,$ and 55. Also shown in each case is the line $m_A = 2m_{\tilde{\chi}_1^0}$, which indicates existence of the A-funnel region in (c) and (d). Color coding same as in Fig. 2.

FIG. 11 (color online). Yukawa ratio y_b/y_τ (at M_{GUT}) versus $\tan\beta$. Color coding same as in Fig. 2.

Finally, as discussed earlier, we have not imposed b-τ Yukawa unification in this paper. For completeness, we plot in Fig. 11 the ratio y_b/y_τ, evaluated at M_{GUT}, versus $\tan\beta$. For the parameter space we have considered this ratio turns out to be $\lesssim 3/4$. It is amusing to note that the value $2/3$ for this ratio, which contains phenomenologically viable points, can be obtained from Eq. (6) by setting $y \approx 0$.

V. CONCLUSION

We have generalized the CMSSM parameterization to one which seems more suited for SU(5) models by replacing the universal sfermion mass m_0 with two independent sfermion masses, $m_{\bar{5}}$ and m_{10}, corresponding to the five- and ten-dimensional representations of SU(5). We have identified some of the parameter space that is allowed,
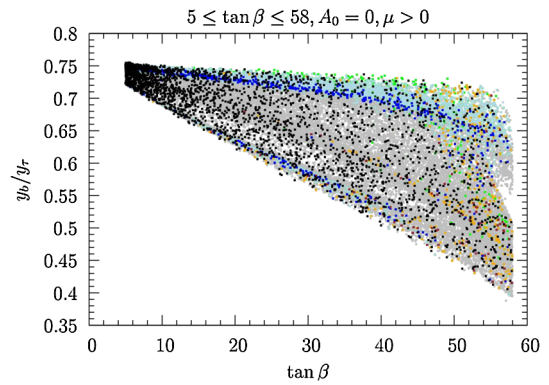
after taking into account a variety of experimental constraints. For points chosen from the allowed parameter space, we have shown that the resultant sparticle mass spectrum can be quite different from the one obtained in the CMSSM, and this difference can be tested at the LHC. With the sparticle masses precisely measured, we can employ them as a tool to probe the underlying GUT using RGEs. This SU(5) inspired version of the CMSSM shows separate unification of sfermion masses in the $\bar{5}$- and 10-dimensional representations.

[1] A. H. Chamseddine, R. L. Arnowitt, and P. Nath, Phys. Rev. Lett. **49,** 970 (1982); R. Barbieri, S. Ferrara, and C. A. Savoy, Phys. Lett. **119B,** 343 (1982); L. J. Hall, J. D. Lykken, and S. Weinberg, Phys. Rev. D **27,** 2359 (1983); E. Cremmer, P. Fayet, and L. Girardello, Phys. Lett. **122B,** 41 (1983); N. Ohta, Prog. Theor. Phys. **70,** 542 (1983).

[2] For recent discussions and additional references see L. Roszkowski, R. Ruiz de Austri, and R. Trotta, J. High Energy Phys. 07 (2007) 075; A. Belyaev, S. Dar, I. Gogoladze, A. Mustafayev, and Q. Shafi,

arXiv:0712.1049; D. Feldman, Z. Liu, and P. Nath, J. High Energy Phys. 04 (2008) 054; J. R. Ellis, K. A. Olive, and P. Sandick, J. High Energy Phys. 08 (2008) 013; F. Feroz, B. C. Allanach, M. Hobson, S. S. AbdusSalam, R. Trotta, and A. M. Weber, J. High Energy Phys. 10 (2008) 064; G. Barenboim, P. Paradisi, O. Vives, E. Lunghi, and W. Porod, J. High Energy Phys. 04 (2008) 079; J. L. Kneur and N. Sahoury, Phys. Rev. D **79,** 075010 (2009); H. Baer and X. Tata, arXiv:0805.1905.

[3] G. Hinshaw *et al.* (WMAP Collaboration), Astrophys. J.

Suppl. Ser. **180**, 225 (2009).

[4] R. Trotta, F. Feroz, M. P. Hobson, L. Roszkowski, and R. Ruiz de Austri, J. High Energy Phys. 12 (2008) 024; F. Feroz, B. C. Allanach, M. Hobson, S. S. AbdusSalam, R. Trotta, and A. M. Weber, J. High Energy Phys. 10(2008) 064.

[5] S. Profumo, Phys. Rev. D **68**, 015006 (2003); B. Ananthanarayan and P. N. Pandita, Int. J. Mod. Phys. A **22**, 3229 (2007).

[6] S. P. Martin and M. T. Vaughn, Phys. Rev. D **50**, 2282 (1994); **78**, 039903(E) (2008).

[7] H. Baer, F. E. Paige, S. D. Protopopescu, and X. Tata, arXiv:hep-ph/0001086.

[8] J. Hisano, H. Murayama, and T. Yanagida, Nucl. Phys. **B402**, 46 (1993); Y. Yamada, Z. Phys. C **60**, 83 (1993); J. L. Chkareuli and I. G. Gogoladze, Phys. Rev. D **58**, 055011 (1998).

[9] D. M. Pierce, J. A. Bagger, K. T. Matchev, and R.-j. Zhang, Nucl. Phys. **B491**, 3 (1997).

[10] L. E. Ibanez and G. G. Ross, Phys. Lett. **110B**, 215 (1982); K. Inoue, A. Kakuto, H. Komatsu, and S. Takeshita, Prog. Theor. Phys. **68**, 927 (1982); **70**, 330(E) (1983); L. E. Ibanez, Phys. Lett. **118B**, 73 (1982); J. R. Ellis, D. V. Nanopoulos, and K. Tamvakis, Phys. Lett. **121B**, 123 (1983); L. Alvarez-Gaume, J. Polchinski, and M. B. Wise, Nucl. Phys. **B221**, 495 (1983).

[11] W. M. Yao *et al.*, J. Phys. G **33**, 1 (2006).

[12] Tevatron Electroweak Working Group and CDF Collab-

oration and D0 Collaboration, arXiv:0803.1683.

[13] H. Baer, C. Balazs, and A. Belyaev, J. High Energy Phys. 03 (2002) 042; H. Baer, C. Balazs, J. Ferrandis, and X. Tata, Phys. Rev. D **64**, 035004 (2001).

[14] L. J. Hall, R. Rattazzi, and U. Sarid, Phys. Rev. D **50**, 7048 (1994). For a recent discussion see W. Altmannshofer, D. Guadagnoli, S. Raby, and D. M. Straub, Phys. Lett. B **668**, 385 (2008), and references therein.

[15] J. R. Ellis and M. K. Gaillard, Phys. Lett. **88B**, 315 (1979).

[16] C. Panagiotakopoulos and Q. Shafi, Phys. Rev. Lett. **52**, 2336 (1984).

[17] L. Roszkowski, R. Ruiz de Austri, and R. Trotta, J. High Energy Phys. 07 (2007) 075.

[18] D. S. Akerib *et al.* (CDMS Collaboration), Phys. Rev. Lett. **96**, 011302 (2006); Z. Ahmed *et al.* (CDMS Collaboration), Phys. Rev. Lett. **102**, 011301 (2009).

[19] J. Angle *et al.* (XENON Collaboration), Phys. Rev. Lett. **100**, 021303 (2008).

[20] J. Hisano, K. Kawagoe, R. Kitano, and M. M. Nojiri, Phys. Rev. D **66**, 115004 (2002).

[21] S. Schael *et al.*, Eur. Phys. J. C **47**, 547 (2006).

[22] T. Aaltonen *et al.* (CDF Collaboration), Phys. Rev. Lett. **100**, 101802 (2008).

[23] E. Barberio *et al.* (Heavy Flavor Averaging Group (HFAG) Collaboration), arXiv:0704.3575.

[24] G. W. Bennett *et al.* (Muon G-2 Collaboration), Phys. Rev. D **73**, 072003 (2006).